NJC

Accepted Manuscript

This is an *Accepted Manuscript*, which has been through the Royal Society of Chemistry peer review process and has been accepted for publication.

Accepted Manuscripts are published online shortly after acceptance, before technical editing, formatting and proof reading. Using this free service, authors can make their results available to the community, in citable form, before we publish the edited article. We will replace this *Accepted Manuscript* with the edited and formatted *Advance Article* as soon as it is available.

You can find more information about *Accepted Manuscripts* in the Information for Authors.

Please note that technical editing may introduce minor changes to the text and/or graphics, which may alter content. The journal's standard Terms & Conditions and the Ethical guidelines still apply. In no event shall the Royal Society of Chemistry be held responsible for any errors or omissions in this *Accepted Manuscript* or any consequences arising from the use of any information it contains.

ROYAL SOCIETY OF CHEMISTRY

www.rsc.org/njc

Table of Contents (TOC)

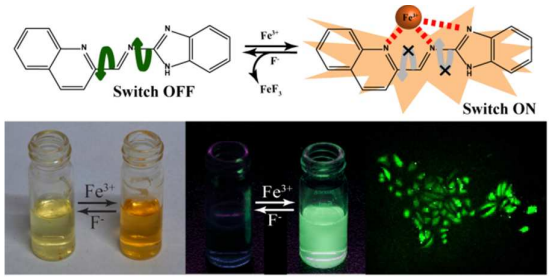

A quinoline functionalized fluorophore exhibited high selectivity towards Fe^{3+} ions and the ligand-metal complex shows excellent selectivity towards F^- ions.

Journal Name

RSCPublishing

ARTICLE

A simple and efficient Fluorophoric probe for dual sensing of Fe^{3+} and F^-: Application to bioimaging in native cellular iron pool and live cell

Cite this: DOI: 10.1039/x0xx00000x

Received 00th January 2012,
Accepted 00th January 2012

DOI: 10.1039/x0xx00000x

www.rsc.org/

Chirantan Kar[a], Soham Samanta[a], Sandipan Mukherjee[b], Barun K. Datta[a], Aiyagari Ramesh*[b] and Gopal Das*[a],

A new quinoline functionalized fluorophoric Schiff base **L_1** was synthesized and it's colorimetric and fluorescence responses toward various metal ions in mixed aqueous media were explored. The ligand exhibited high selectivity towards Fe^{3+} in presence of large excess of other competing ions with certain observable optical and fluorescence changes. These spectral changes are significant enough in the visible region of the spectrum and thus enable naked eye detection. The efficiency of **L_1** in detecting Fe^{3+} ions was also checked in presence of relevant complex biomacromolecules viz. met-hemoglobin, fetal bovine serum and human serum albumin. **L_1** was also found to be enough sensitive for visual detection of Fe^{3+} ions in native iron pools of banana pith. Studies revealed that **L_1-Fe** complex formation is fully reversible in presence of fluoride anion with very high selectivity. Further, fluorescence microscopic studies demonstrated that compound **L_1** could also be used as an imaging probe for detection of uptake of these ions in model human cells. This selective sensing behaviour of **L_1** towards Fe^{3+} was explained via CHEF process where theoretical calculations also supported the premise.

Introduction

The general basis of designing a molecular sensor for selective recognition of different species depends upon host guest interaction promoted by hydrogen bonding, electrostatic force, metal-ligand coordination, hydrophobic and van der Waals interaction.[1-3] In recent years, development of novel colorimetric and fluorescent sensors of biologically relevant metal ions has been extensively pursued because of the advantages of high selectivity, sensitivity, non-destructive analysis, simple instrumentation and their potential applications in analytical chemistry and biomedical sciences. Among biologically important metals, iron is one of the most abundant essential elements found in human body and is critical to sustain important physiological processes.[4-8] Iron provides the oxygen-carrying capacity of heme and acts as a cofactor in many enzymatic reactions. It plays key roles in numerous biological processes at cellular level ranging from oxygen metabolism and electron-transfer processes to DNA and RNA synthesis.[9,10] Iron is indispensable for most organisms, and its deficiency as well as overload can lead to detrimental consequences.[11-14] Given the physiological implications of iron, its detection assumes considerable significance. It is generally believed that probes with a fluorescence enhancement signal upon interaction with analyte are desirable. However, Fe^{3+} ion is well-known as a fluorescence quencher due to its paramagnetic nature, and most of the reported Fe^{3+} receptors, such as analogues of ferrichromes or siderophores, undergo a fluorescence quenching when bound with Fe^{3+}.[15-17] Therefore, the development of new fluorescent Fe^{3+} indicators, especially those that exhibit selective Fe^{3+}-amplified emission, is still a challenge.[18,19]

Development of selective and efficient signaling units for detection of various chemically and biologically important anions has also attained significant interest.[20,21] In this context, the role of fluoride in human health is well recognized. While at low concentration fluoride plays a beneficial role in treating osteoporosis and protecting dental health, it is apparently toxic at higher doses.[22] Over the years, high concentration of fluoride anion in the environment and in drinking water has been related to the occurrence of several types of ailment in humans.[22-24] Hence there is a growing need of developing systems capable of recognition, binding and/or sensing of fluoride in a competitive and aqueous environment. Although, the significance of fluoride anion has led to efforts to develop fluoride sensors over the past decade,[25-32] but due to its high enthalpy of hydration fluoride sensing in aqueous solution has proved to be very difficult and molecular systems that can sense fluoride anions in aqueous systems are scarce.[33,34]

In conjunction with visible absorbance signals, a fluorescence response in the visible region would be an added advantage with regard to sensitivity, specificity, and fast response real-time monitoring[35-37] of cations and anions over the methods which are based on a single kind of optical response. From the recent literature it is apparent that considerable efforts have been made for selective sensing of Iron[4-8] and fluoride[25-32] ions with absorbance and emission in the visible region. However,

the optical detection of these analytes in aqueous/mixed aqueous media is still rare. Together with their high sensitivity and efficiency, fluorescent receptors which are soluble in aqueous/mixed solvent offer an added advantage in cellular analysis.[38,39] In addition, the optical detection of analytes inside living organisms helps to probe their site of action and physiological functions.[40,41]

Schiff bases are well known as ion carriers and for the formation of stable complexes with transition metal ions. The structure of Schiff bases render geometric and cavity control of host-guest complexation and produce exceptional selectivity, sensitivity and stability for a specific ion. Consequently, Schiff base complexes have attracted increasing attention in the area of ionic binding. Quinoline aldehyde based Schiff base are noteworthy and their transition metal complexes are extensively studied for their proteasome inhibiting activity in human cancer cells.[42] The quinoline scaffold having a formyl/acetyl group adjacent to heterocyclic nitrogen can be easily appended with other fluorophore bearing amino groups to yield Schiff base compounds, which can form complexes with a wide range of transition metal ions. Several studies have demonstrated the use of rationally designed Schiff base ligands for optical sensing of transition metal ions.[43-48]

In view of the biological importance of Fe^{3+} and F^- ions, we have combined the advantage of the characteristics of an UV-Vis response with the sensitivity of a fluorophoric response for the construction of a chemosensor probe (Scheme 1), that may be potentially useful for the detection of Fe^{3+} as well as F^- ions in physiological pH. In our continuous endeavour to design sensor for various analytes,[49-56] herein, we report the metal and anion sensing capabilities of a quinoline functionalized fluorophoric Schiff base ligand **L_1**(Scheme 1) and the absorption and fluorescence behaviour of **L_1** upon metal complexation, both in solution as well as in live cells.

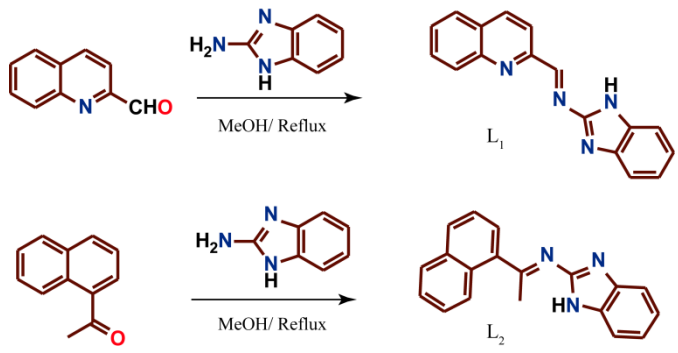

Scheme 1 Synthetic scheme of **L_1** and **L_2**.

Experimental Section

General Information and Materials.

All the materials for synthesis were purchased from commercial suppliers and used without further purification. The absorption spectra were recorded on a Perkin-Elmer Lamda-25 UV-visible spectrophotometer using 10 mm path length quartz cuvettes in the range of 250–500 nm wavelengths, while the fluorescence measurements were carried on a Horiba Fluoromax-4 spectrofluorometer using 10 mm path length quartz cuvettes with a slit width of 5 nm at 298 K. The mass spectra were obtained using Agilent Technologies 6520 Accurate mass spectrometer. NMR spectra were recorded on a Varian FT-400 MHz instrument. The chemical shifts were recorded in parts per million (ppm) on the scale. The following abbreviations are used to describe spin multiplicities in ^{1}H NMR spectra: s = singlet; d = doublet; t = triplet; m= multiplet. Elemental analyses were performed with a Perkin Elmer 2400 elemental analyser.

Detection of the Fe^{3+} in fetal blood serum

For determination of Fe^{3+} in fetal bovine serum, the serum was firstly treated with trichloroacetic acid (TCA) to release Fe^{3+} from protein according to a reported procedure.[57] 4 mL of 20% TCA was added to 4 mL serum, and then the mixture was stirred and heated to 90°C for 15min. After cooling, the mixture was sonificated for 2 min. The protein precipitate was removed by centrifugation at 10000 rpm for 10 min. The supernatant was used for the Fe^{3+} assay. Aliquots of the above deproteined serum sample (0 µL, 10 µL, 20 µL, 30 µL, 40 µL, 50 µL, g = 60 µL, 70 µL, 80 µL, 90 µL, 100 µL) were added to 1 mL solution of **L_1** in CH_3CN/aqueous HEPES buffer (1 mM, pH 7.3; 1:4 v/v). After that the resulting solution is incubated at room temperature for 30 min, and then the fluorescence experiments with the following samples are performed.

Imaging of banana pith

The freshly collected banana pith was sectioned and washed carefully with HEPES buffer (pH 7.2). Then the sections were treated with ligand solution (25 µM), washed and then photographed. Another set of sections were treated first with EDTA to chelate the iron present in the pith and then with ligand, and finally photographed.

Synthesis of L_1

Quinoline 2-carboxaldehyde (471 mg, 3 mmol) and 2-amino benzimidazole (400 mg, 3 mmol) were dissolved in 20 mL of methanol. To this was added approximately 2 drops of acetic acid, and the resulting solution was refluxed for 10 h. An yellowish precipitate was found. The reaction mixture was allowed to attain room temperature, and then the precipitate was collected through filtration. The residue was washed thoroughly with methanol to isolate **L_1** in pure form with 43% yield. ^{1}H NMR [400 MHz, DMSO-d_6, $SiMe_4$, J (Hz), δ (ppm)]: 9.52 (1H, s), 8.53 (1H, t, J=9.2), 8.42 (1H, d, J=8.4), 8.34 (1H, d, J=8.4), 8.19 (1H, m), 8.09 (1H, t, J=6.8), 7.99 (1H, d, J=8.4), 7.72-7.93 (3H, m), 7.62 (1H, t, J=7.2), 6.153 (1H, s). ^{13}C NMR [100 MHz, DMSO-d_6, $SiMe_4$, δ (ppm)]: 165.12, 157.91, 155.36, 154.76, 138.62, 138.13, 137.49, 130.69, 130.15, 129.48, 128.84, 128.05, 127.66, 119.94, 119.31, 112.30, 111.70. ESI-MS (positive mode, m/z). Calcd for $C_{17}H_{12}N_4$: 272.106. Found: 273.113 ($M + H^+$). Anal. Calcd. for $C_{17}H_{12}N_4$ (272.106): C 74.98, H 4.44, N 20.58; found C 74.89, H 4.35, N 20.65.

Synthesis of L_2

L_2 was synthesized following a method previously reported in literature.[58]

UV−Vis and fluorescence spectral studies

Stock solutions of various ions (1×10^{-3} mol·L^{-1}) were prepared in deionized water. A stock solution of **L_1** (1×10^{-3} mol·L^{-1}) was prepared in DMSO. The solution of **L_1** was then diluted to 1×10^{-5} mol·L^{-1} with CH_3CN/aqueous HEPES buffer (1 mM, pH 7.3; 1:4 v/v). The FBS (Fetal bovine serum) samples were kept at low temperature (-20 °C) for storage. 50 µL of serum was dissolved in 1.5 mL of de-ionized water and

used as stock solution. The stock solution for HSA (Human Serum Albumin) protein was prepared at a concentration of 1 mg mL^{-1} in de-ionized water. Experiments could not be performed beyond this concentration with either the serum or HSA protein due to their precipitation. During titration experiment with increasing amount of metHb, the concentration of metHb (*met*-haemoglobin) inside cuvette is maintained from 0 to 4 μM. In titration experiments with increasing amount of Fe^{3+}, each time a 1×10^{-3} L solution of $\mathbf{L_1}$ (1×10^{-5} mol·L^{-1}) was filled in a quartz optical cell of 1 cm optical path length, and the ion stock solutions were added into the quartz optical cell gradually by using a micro-pipet. Spectral data were recorded at 1 min after the addition of the ions. In selectivity experiments, the test samples were prepared by placing appropriate amounts of the anions/cations stock into 2 mL of solution of $\mathbf{L_1}$ (2×10^{-5} mol·L^{-1}). For fluorescence measurements, excitation was provided at 405 nm and emission was collected from 420 to 600 nm.

Evaluation of the binding constant for the formation of L_1-Fe complex

Receptor $\mathbf{L_1}$ with an effective concentration of 10.0×10^{-6} M in an acetonitrile/aqueous HEPES buffer (1 mM; 1:4, v/ v; pH 7.3) was used for the emission titration studies with a Fe^{3+} solution. A stock solution of $Fe(NO_3)_3$, having a concentration of 0.2×10^{-3} M in an acetonitrile/aqueous HEPES buffer (1:4, v/v; pH 7.3) solution was used. The effective Fe^{3+} concentration was varied between 0 and 30×10^{-6} M for this titration. The solution pH was adjusted to 7.3 using an aqueous HEPES buffer solution having an effective concentration of 1 mM.

Binding constant

The binding constant for the formation of the respective complexes were evaluated using the Benesi−Hildebrand (B−H) plot (eq 1).[59]

$$1/(I-I_0)=1/\{K(I_{max}-I_0)C\}+1/(I_{max}-I_0) \quad (1)$$

I_0 is the emission intensity of $\mathbf{L_1}$ at emission maximum ($\lambda = 472$ nm), I is the observed emission intensity at that particular wavelength in the presence of a certain concentration of the metal ion (C), I_{max} is the maximum emission intensity value that was obtained at $\lambda = 472$ nm during titration with varying metal ion concentration, K is the binding constant (M^{-1}) and was determined from the slope of the linear plot, and C is the concentration of the Fe^{3+} ion added during titration studies.

Detection limit

The detection limit was calculated based on the fluorescence titration. The fluorescence emission spectrum of $\mathbf{L_1}$ was measured independently for ten times and the standard deviation of blank measurement was achieved. To gain the slope, the ratio of the emission intensity at 472 nm was plotted as a concentration of Fe^{3+}.

The detection limit was calculated using the following equation:

$$\text{Detection limit} = 3\sigma/k \quad (2)$$

where σ is the standard deviation of blank measurement, k is the slope between the ratio of emission intensity versus [Fe^{3+}].

Cytotoxic effect on HeLa cells

The cytotoxic effect of compound $\mathbf{L_1}$ and $\mathbf{L_1}$-**Fe**complex was determined by performing a standard MTT assay following the manufacturer instruction (Sigma-Aldrich, MO, USA). HeLa cells (human cervical carcinoma cell line) were initially cultured in a 25 cm^2 tissue culture flask in Dulbecco's Modified Eagle Medium (DMEM) supplemented with 10% (v/v) fetal bovine serum (FBS), penicillin (100 μg/mL) and streptomycin (100 μg/mL) in a CO_2 incubator. For MTT assay, cells were seeded into 96-well plates (approximately 10^4 cells per well) and various concentrations of compound $\mathbf{L_1}$ and $\mathbf{L_1}$-**Fe** complex (15, 30, 45 and 60 μM) made in DMEM were added to the cells and incubated for 24 h. Solvent control samples (cells treated with DMSO alone) and cells treated with $Fe(NO_3)_3$ alone were also included in parallel sets. Following incubation, the growth media was carefully aspirated and fresh DMEM containing MTT solution was added. The plate was further incubated for 3-4 h at 37°C. Subsequently, the supernatant was removed and the insoluble colored formazan product was solubilized in DMSO and its absorbance was measured in a microtitre plate reader (Infinite M200, TECAN, Switzerland) at 550 nm. The assay was performed in six sets for each concentration of compound $\mathbf{L_1}$ and $\mathbf{L_1}$-**Fe** complex. Data analysis and calculation of standard deviation was performed with Microsoft Excel 2010 (Microsoft Corporation, USA).

Cell imaging studies

HeLa cells were propagated in Dulbecco's Modified Eagle Medium (DMEM) supplemented with 10% (v/v) fetal bovine serum, penicillin (100 μg/mL), and streptomycin (100 μg/mL). Cells were maintained under a humidified atmosphere of 5% CO_2 and at 37 °C incubator as mentioned before. For imaging studies, cells were seeded into a 6 well plate and incubated at 37^0 C in a CO_2 incubator for 3 days. Subsequently, cells were washed thrice with sterile phosphate buffered saline (pH 7.4) and incubated with 10 μM $\mathbf{L_1}$ in DMEM at 37 °C for 1 hr in a CO_2 incubator and observed under an epifluorescence microscope (Nikon eclipse Ti). The cells were again washed thrice with sterile PBS (pH 7.4) to remove the free $\mathbf{L_1}$, and then incubated in the same with 20 μM $Fe(NO_3)_3$ for 1 hr and again the cell images were recorded using an epifluorescence microscope. The cells were then treated with 30 μM of KF solution and after incubation for 1hr the cells were washed with sterile PBS thrice to remove free compound and ions and then fluorescence microscopic images were recorded.

Results and discussion

In this article we have discussed the design and application of a quinoline functionalized fluorophoric imine $\mathbf{L_1}$ which can selectively bind and sense Fe^{3+} ions in presence of other interfering metal ions. $\mathbf{L_1}$ can be easily synthesized by refluxing Quinoline 2-carboxaldehyde and 2-amino benzimidazole in methanol. The synthetic procedure of $\mathbf{L_1}$ is described in scheme 1.

UV-Vis spectroscopic studies of L_1 in presence of Fe^{3+}

The interaction of $\mathbf{L_1}$ with various guest species was ascertained by UV-vis absorption spectroscopic analysis. As observed in Figure 1A, ligand $\mathbf{L_1}$ in CH_3CN/aqueous HEPES buffer (1 mM, pH 7.3; 1:4 v/v**)** shows an absorption maximum at 283 nm, which may be ascribed to intra-molecular π-π* charge transfer (CT) transition. Addition of increasing amounts of Fe^{3+} ions resulted in an increase in absorption (figure 1B), with a visual change in color from yellowish to reddish (Figure 1A inset). This may be accounted by the change in the orientation of the aromatic fluorophoric units in the ligand.

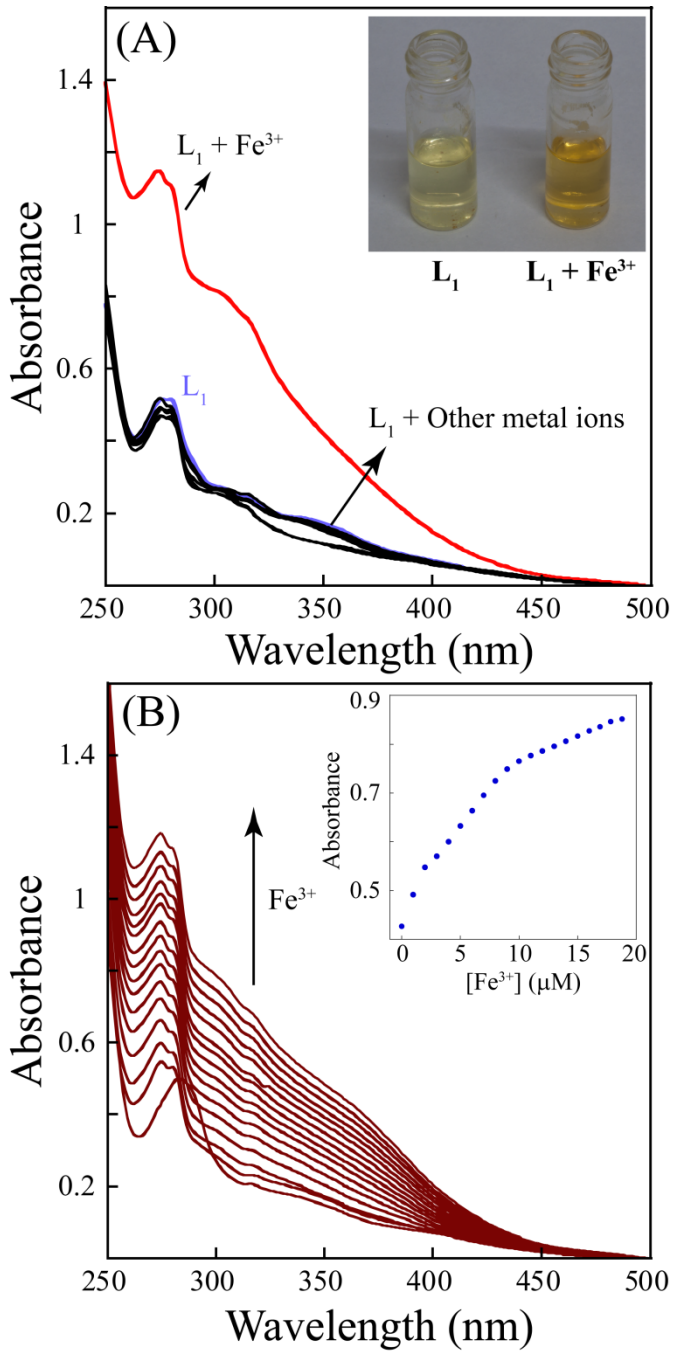

Fig. 1 (A) Changes of the UV-vis spectra of ligand L_1 (10 μM) observed upon addition of Fe^{3+} (1 equivalent) and other metal ions (perchlorate or nitrate salts of Na^+, K^+, Ca^{2+}, Mg^{2+}, Cr^{3+}, Hg^{2+}, Cu^{2+}, Pb^{2+}, Zn^{2+}, Fe^{2+}, Al^{3+}, Ni^{2+}, Co^{2+}, Cd^{2+}, and Ag^+) (10 equivalent) in mixed solvent system. **Inset**: Visual change in color of L_1 after addition of Fe^{3+} (B) UV-Vis titration spectra of L_1 (10 μM) upon incremental addition of $Fe(NO_3)_3$. **Inset:** Changes in the UV-Vis absorbance at 274 nm with incremental addition of Fe^{3+}.

To appropriately determine the selectivity of L_1 towards Fe^{3+}, we examined the absorption behaviour of L_1 in presence of various metal ions (Na^+, K^+, Ca^{2+}, Mg^{2+}, Cr^{3+}, Hg^{2+}, Cu^{2+}, Pb^{2+}, Zn^{2+}, Fe^{2+}, Al^{3+}, Ni^{2+}, Co^{2+}, Cd^{2+}, and Ag^+) as their perchlorate or nitrate salts. However, no change in absorption band of compound L_1 in the presence of other metal ions was observed.

Fluorescence spectroscopic studies of L_1 in presence of Fe^{3+}

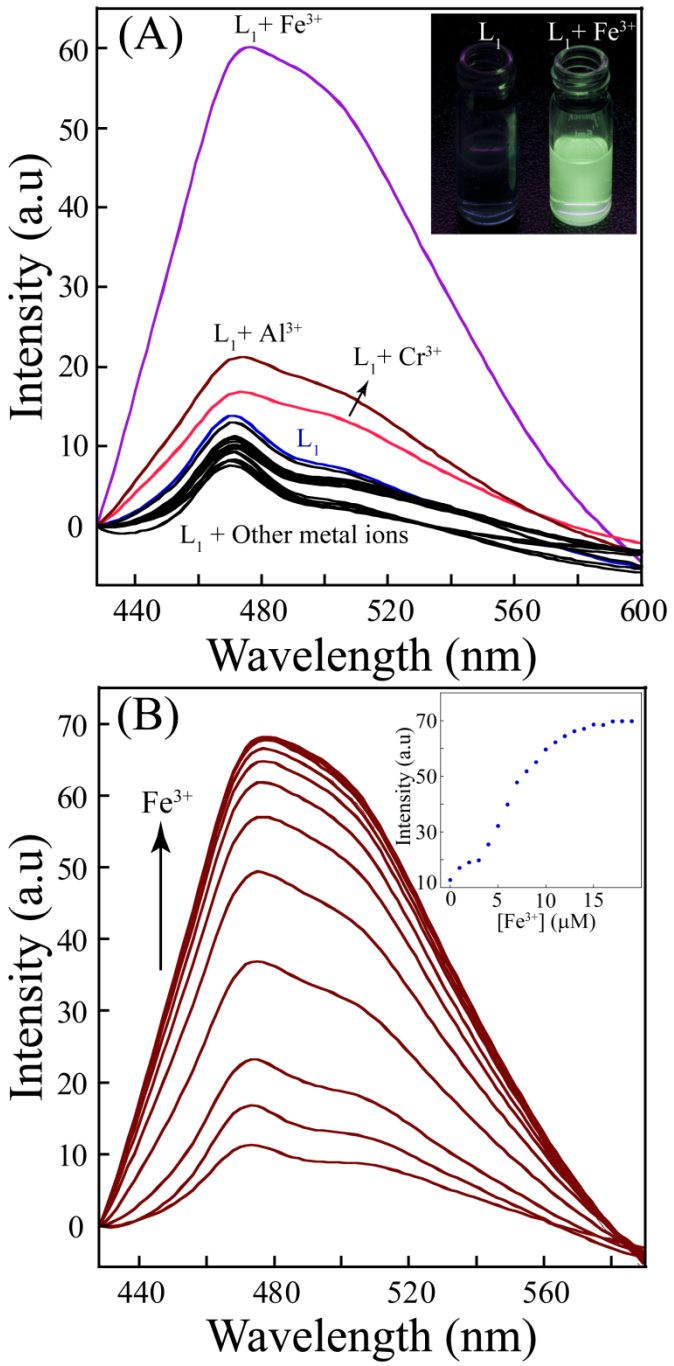

Fig. 2 (A) Changes of the fluorescence emission of receptor L_1 (10 μM) observed upon addition of Fe^{3+} (1 equivalent) and other metal ions (perchlorate or nitrate salts of Na^+, K^+, Ca^{2+}, Mg^{2+}, Cr^{3+}, Hg^{2+}, Cu^{2+}, Pb^{2+}, Zn^{2+}, Fe^{2+}, Al^{3+}, Ni^{2+}, Co^{2+}, Cd^{2+}, and Ag^+) (10 equivalent) in mixed solvent system. **Inset:** Visual change in fluorescenc emission of L_1 after addition of Fe^{3+} (B) Fluorescence titration spectra of L_1 (10 μM) upon incremental addition of 2 equiv. of $Fe(NO_3)_3$ (λ_{ex}= 405 nm). **Inset:** Changes in the fluorescence intensity at 472 nm with incremental addition of Fe^{3+}.

The selectivity of L_1 for Fe^{3+} was also studied by fluorescence emission spectroscopy. As evident from Figure 2A, a solution of L_1 (10.0×10^{-6} M) exhibited a low intensity emission maxima at 472 nm when excited at 405 nm. Addition of Fe^{3+} to

this receptor solution induced a significant increase in the fluorescence response with a redshift of the emission maxima to 478 nm. The spectral change is also accompanied by a visual change of the fluorescence emission from colorless to green (Figure 2A inset). It can also be observed from Figure 2A that the metal-ligand binding induced fluorescence intensity enhancement of **L_1** was significantly selective towards Fe^{3+} ions. Under the same conditions as used above for Fe^{3+}, we also tested the fluorescence response of **L_1** to other metal ions such as Na^+, K^+, Ca^{2+}, Mg^{2+}, Cr^{3+}, Hg^{2+}, Cu^{2+}, Pb^{2+}, Zn^{2+}, Fe^{2+}, Al^{3+}, Ni^{2+}, Co^{2+}, Cd^{2+}, and Ag^+. No significant fluorescence change of **L_1** occurred even in the presence of excess of these metal ions. To gain an insight of the properties of **L_1** as a receptor for Fe^{3+}, a titration of the receptor was performed with increasing concentration of Fe^{3+}. As evident in Figure 2B the fluorescence intensity of a 10 μM solution of **L_1** was enhanced with gradual addition of Fe^{3+} ions, which also confirmed that receptor **L_1** exhibited a high sensitivity toward Fe^{3+}, with near about 6 fold increase of its fluorescence intensity upon addition of only 2.0 equiv of Fe^{3+} ions. The 1:1 stoichiometry of the **L_1**-Fe^{3+} was established from the measurements of emission intensity as a function of Fe^{3+} concentration (inset in Figure 2B), where a clear bend of the curve can be observed at 1 equivalent of added Fe^{3+}.

This stoichiometry was also confirmed with the help of job's plot (Supplementary data, Fig. S1) and further corroborated by ESI-MS studies (Supplementary data, Fig. S2), which indicated the presence of molecular-ion peaks at m/z 542.069 and 199.5372 corresponding to the mass of $[L_1+Fe+5H_2O+2NO_3]^+$ and $[L_1+Fe+3H_2O+OH]^{2+}$ respectively. The binding constant for the formation of **L_1-Fe** complex was calculated on the basis of change in emission at 472 nm by considering a 1:1 binding stoichiometry (Supplementary data, Fig. S3). The binding constant (*K*) determined by the B-H method was found to be 2.6×10^4 M^{-1}. It is significant to mention that the detection limit of **L_1** for Fe^{3+} ions was found to be 4 μM, which was significantly lower than the U.S. EPA maximum allowable limit for Fe^{3+} ions (0.3 mg/L) in drinking water.

The change in emission spectral behavior of **L_1** in presence of Fe^{3+} can be explained by chelation-enhanced fluorescence (CHEF). As **L_1** is a biheteroaryl system so the quinoline and the benzimidazole rings may not be perfectly planar, metal coordination helps the rings to become more planar and in turn enhance the resonance. When both the part of the ligand is in a non-planar orientation, the fluorescence is quenched due to lack of internal charge transfer throughout the system. But in presence of a suitable metal cation the lone pairs of electron from the imine, quinoline and benzimidazole nitrogen may participate in metal-ligand coordination bonding. Due to metal assisted planar structure of the metal-ligand coordination complex, the possibility of internal charge transfer throughout the π-system increases; leading to a highly conjugated geometry and a radical enhancement of the fluorescence intensity.

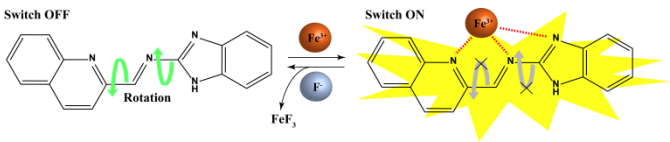

Scheme 2 Fe^{3+}-induced fluorescence switch OFF→ON of the receptor **L_1**.

To further verify the significance and involvement of the quinoline lone pair in Fe^{3+} sensing event, we have synthesized a control compound **L_2**. **L_2** has a similar structure to **L_1** but in place of a quinoline moiety in **L_1** a naphthalene moiety is present in **L_2**. Fluorescence emission studies with **L_2** revealed that there was no significant change in the emission intensity upon addition of an excess amount of Fe^{3+} to a solution containing **L_2** (Supplementary data, Fig. S4), which suggested that in absence of quinoline moiety, Fe^{3+} binding event did not occur. Based on these findings, it can be presumed that the chelating mode of binding to Fe^{3+} by **L_1** restrict the molecule in a planar geometry which extends the conjugation of the π-electron throughout the molecule, which in turn trigger a switch ON response in the fluorescence spectra via chelation-enhanced fluorescence (CHEF) mechanism (Scheme 2).

To further understand the relationship between the structural changes from **L_1** to it's complex with Fe^{3+} and the optical response of **L_1** to Fe^{3+} we carried out density functional theory (DFT) calculations with B3LYP/631+G(d,p) method basis set using the Gaussian 03 program. The optimized geometry and the highest occupied molecular orbital (HOMO) and the lowest unoccupied molecular orbital (LUMO) of L_1 and its Fe^{3+} complex are presented in Figure 3. The slight lowering in the HOMO to LUMO energy gap in **L_1-Fe** complex compared to free **L_1** probably causing the small red shift in the emission spectra of **L_1** when $Fe^{3+}$was added to it. Selected orbitals and their corresponding energies were provided in supplementary data which might have been playing vital role in the optical spectral outcome (Fig. S5). The substantial decrease in the total energy (From -23784.90 eV of L_1 to -66459.76 eV of L_1-Fe^{3+} complex) of L_1 on complexation with Fe^{3+} suggests that the formed L_1-Fe^{3+} complex is highly stable which is probably initiating the spectral out come through CHEF mechanism.

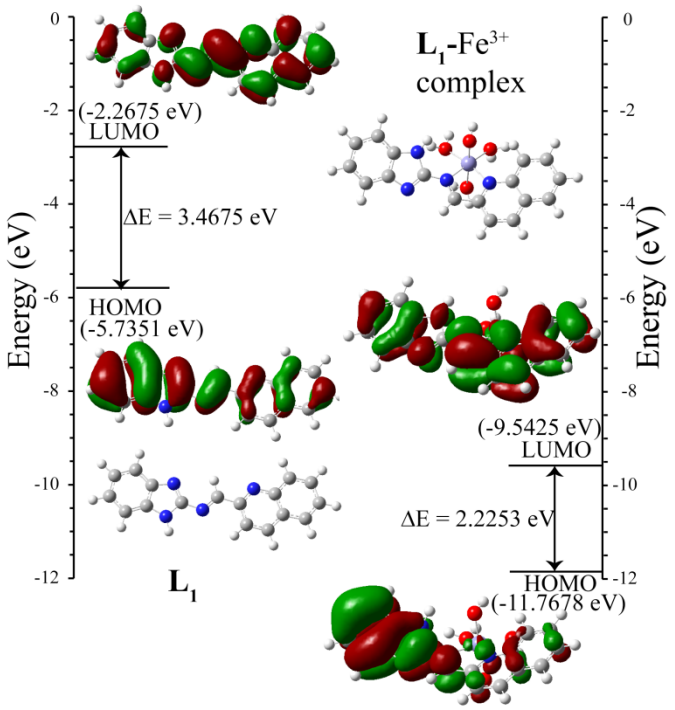

Fig. 3 Energy diagrams of HOMO and LUMO orbitals of L_1 and the L_1–Fe^3 complex calculated at the DFT level using a B3LYP/6-31+G(d,p) basis set.

The potential utility of **L_1** in sensing Fe^{3+} ion was also checked in complex environmental as well as biological samples. Tap, lake and river water were collected from laboratory, the pool of serpentine lake in IIT Guwahati, and Brahmaputra river

(Kamrup district, Assam), respectively. Fe^{3+} (1-10 μM) were spiked into these samples before the addition of $\mathbf{L_1}$ (10 μM). The results of the fluorescence spectroscopic measurements observed from this study are depicted in Figure 4A The fluorescence intensities were also proportional to the concentrations of Fe^{3+} in the range of 1–10 μM (lower than current aquatic life standard in India, which is 1.0 mg/l based on toxic effects).[60] Therefore, the ligand $\mathbf{L_1}$ can be applied for detection of traces of Fe^{3+} in complex environmental systems.

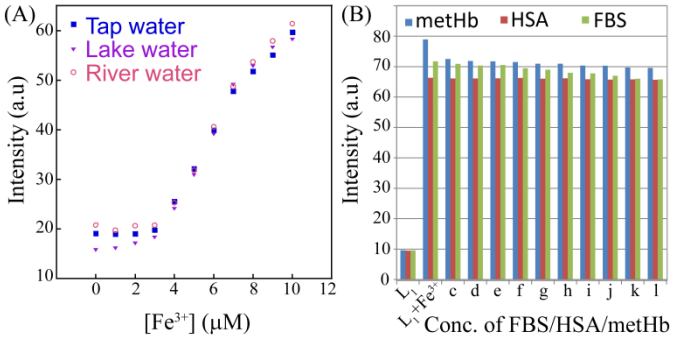

Fig. 4 (A) Change in fluorescence intensities of $\mathbf{L_1}$ (10 μM) at 472 nm wavelength upon continuous addition of Fe^{3+} (0–10 μM) in three natural water samples. (B) Selectivity of $\mathbf{L_1}$ towards Fe^{3+} in the presence of different concentrations of HSA protein, blood serum (FBS) and *met*-Hemoglobin in mixed solvent system; **a** = $\mathbf{L_1}$ (10 μM) + 0 μL protein, **b** = $\mathbf{L_1}$ (10 μM) + Fe^{3+} (10 μM) + 0 μL protein, **c**-**l** = incremental addition of different proteins (10 μL -100 μL) to the solution **b**.

The involvement of peroxides and free radicals in the different reactions inside human body can enhance the oxidation of the oxyheme form, resulting in a breakdown of the heme ring and liberation of iron.[61-64] Humans do not have an active iron excretion mechanism, and levels of nontransferrin-bound-iron (NTBI) in excess of the regulated Fe^{3+} concentrations can generate reactive oxygen species (ROS) that can lead to dysfunction of the heart, liver, anterior pituitary, and pancreas. Thus excess iron inside living system is implicated in the etiology of several degenerative diseases.[65,66] Given the significant physiological impact of Fe^{3+} in living system, there is a considerable need of designing sensor probe which can detect Fe^{3+} ions in mammalian body fluid. In this regard we have verified the Fe^{3+} detecting capability of $\mathbf{L_1}$ in presence of plasma protein (HSA), globular protein (*Met*-haemoglobin) and fetal bovine serum (FBS). As evident from figure 4B no change in the fluorescence emission of $\mathbf{L_1}$-**Fe** complex was observed on addition of varying concentrations of *Met*-haemoglobin, Human serum albumin (HSA) and fetal bovine serum (FBS). This indicated the high binding efficiency of $\mathbf{L_1}$ with Fe^{3+} ions over the *met*-haemoglobin, Human serum albumin (HSA) protein and fetal bovine serum. On the other hand, when Fe^{3+} ions were added to the solution of ligand $\mathbf{L_1}$ and *met*-haemoglobin/Human serum albumin (HSA) protein/ fetal bovine serum, the characteristic fluorescence enhancement was observed in the emission intensity at 472nm of $\mathbf{L_1}$ (Supplementary data, Fig. S9). These observations again reiterate the strong interactions of ligand $\mathbf{L_1}$ with Fe^{3+} ions over the biological guests. Kumar *et al.*[67] have reported a fluorescent chemosensor based on calix[4]arene which shows Fe^{3+} selective switch off response in blood serum and different proteinous environment.

The strong potential of $\mathbf{L_1}$ in sensing Fe^{3+} ions are further demonstrated by fluorescence microscope imaging of native iron pools inside plant system. We have particularly chosen banana pith sections as an iron-rich part of banana plant. When these sections were treated with $\mathbf{L_1}$, a strong green emission was observed indicating the presence of Fe^{3+} ions (Figure 5). We have also performed a control experiment where we have treated the banana pith sections with EDTA to chelate the iron present and then treated them with $\mathbf{L_1}$. The control experiment didn't show any increase in green fluorescence of the banana pith sections which concludes that the emergence of the green fluorescence is only due to the formation of $\mathbf{L_1}$-**Fe** complex inside the biological system.

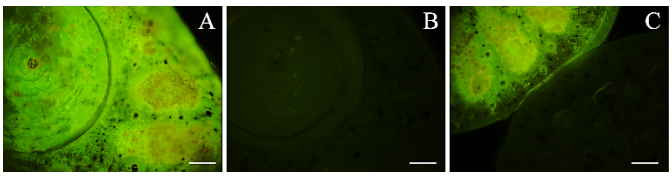

Fig. 5 Fluorescence microscopic photograph of transverse section of (A) banana pith treated with $\mathbf{L_1}$, (B) banana pith treated with EDTA first followed by $\mathbf{L_1}$, (C) banana pith treated with $\mathbf{L_1}$ and banana pith treated with EDTA first followed by $\mathbf{L_1}$ attached together. Scale bar for the images is 200 μm.

UV-Vis spectroscopic studies of L_1-Fe complex in presence of anions

Hence from the above mentioned studies it was evident that $\mathbf{L_1}$ selectively binds with Fe^{3+} to form $\mathbf{L_1}$-**Fe** complex with a distinct change in its optical as well as fluorescence properties. The next endeavor was to ascertain the influence of different anions on the disassembly/dissociation of this metal-ligand complex and their effect on the reversibility of this complex to regenerate $\mathbf{L_1}$**.** The UV-Vis spectroscopic study of the $\mathbf{L_1}$-**Fe** complex was pursued in presence of different anions such as F^-, Cl^-, Br^-, I^-, CN^-, $H_2PO_4^-$, NO_3^-, NO_2^-, SO_4^{2-}, HSO_3^-, and S^{2-}.

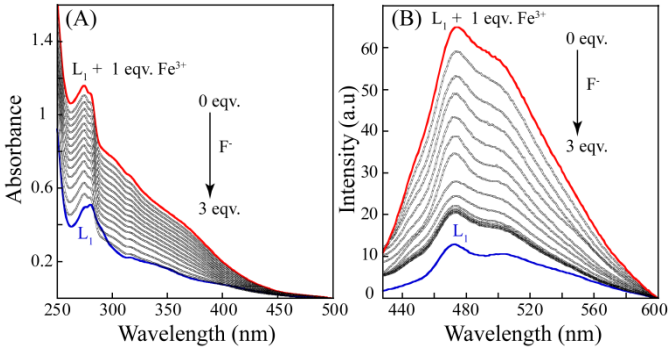

Fig. 6 (A) UV-Vis titration spectra of $\mathbf{L_1}$ (10 μM) with 1 equiv of Fe^{3+} upon addition of sodium fluoride (30 μM) in mixed solvent system. (B) Fluorescence titration spectra (λ_{ex} = 405 nm) of $\mathbf{L_1}$ (10 μM) with 1 equiv of Fe^{3+} upon addition of fluoride (30 μM) ion.

It is worth mentioning that the regeneration of compound $\mathbf{L_1}$ was observed only by adding F^- to the solution containing $\mathbf{L_1}$-**Fe**, whereas other anions failed to demonstrate any significant spectral change. To obtain a comprehensive understanding of the properties of $\mathbf{L_1}$-**Fe** complex in presence of F^- anion, a solution of $\mathbf{L_1}$ in mixed solvent containing 1 equiv. of Fe^{3+} was titrated in presence of increasing amount of fluoride anions. The UV-Vis spectral pattern of the titration spectra (Figure 6A) displayed a reverse trend to the titration curve obtained with

Fe^{3+} (Figure 1B), which provided evidence that ligand **L_1** could be regenerated from the complex in presence of F^-.

Fluorescence spectroscopic studies of L_1-Fe complex in presence of anions

Fluorescence spectroscopy studies of **L_1-Fe** complex in presence of different anions were also pursued. Interestingly it was observed that the emission of **L_1-Fe** complex was completely restored to its native **L_1** state, selectively in presence of fluoride anions. To further verify the fluorescence "ON-OFF'' switching property of the sensor, we have performed fluorescence titration experiment. Initially the fluorescence intensity of the compound **L_1** was enhanced to an adequate level in presence of 1 equiv. of Fe^{3+} ions, the resulting **L_1-Fe** complex was then titrated by addition of increasing amounts of fluoride ions. As evident from Figure 6B the fluorescence intensity of **L_1-Fe** complex decreased with increasing concentration of fluoride anion and on addition of near about 3 equiv. of F^- anion both the intensity and overall pattern of emission spectrum closely resembled those of compound **L_1** (Figure 2B), so that the fluorescence intensity along with the maximum emission peak were fully regained. After addition of the F^- anion, the fluorescence emission response of the **L_1-Fe** complex was rapid (within 15 sec) and stable and thus the probe was robust and virtually rendered real-time monitoring of the target anion. Thus, the results of the spectroscopic studies indicated that the sensor **L_1** was regenerated during the detection procedure of fluoride anions.
In order to verify the reason of the fluorescence "off–on" property, the mass spectrum of the **L_1-Fe** system is also recorded in presence of F^-. The mass spectrum of the **L_1-Fe** system shows a molecular-ion peak at 542.069, corresponding to the mass of $[L_1 + Fe + 5H_2O + 2NO_3]^+$ (Supplementary data, Fig. S2). While subsequent addition of F^- ions to the above solution gives a molecular ion peak at m/z 273.11 which confirmed the identity of free **L_1** and validated the mechanism of the sensing of fluoride anions (Supplementary data, Fig. S10).

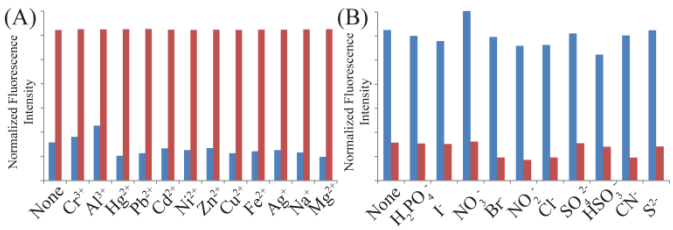

Fig. 7 (A) Normalized fluorescence responses of **L_1** (10 μM) to various cations in mixed solvent system. The blue bars represent the emission intensities of **L_1** in the presence of cations of interest (50 μM). The red bars represent the change of the emission that occurs upon the subsequent addition of Fe^{3+} to the above solution; (B) Normalized fluorescence responses of **L_1-Fe** to various anions in mixed solvent system. The blue bars represent the emission intensities of **L_1-Fe** in the presence of anions of interest (50 μM). The red bars represent the change of the emission that occurs upon the subsequent addition of F^- to the above solution. The intensities were recorded at 472 nm.

The practical applicability of compound **L_1** and **L_1-Fe** complex as a Fe^{3+} and F^- selective fluorescent sensor was addressed by carrying out experiments in the presence of other competing cations and anions, which may interfere in estimation of iron and fluoride (Figure 7). The receptor **L_1** and the **L_1-Fe** complex both exhibited exclusivity and were efficient in their sensing ability of the respective analytes from a competitive environment.

Biological studies of L_1 in presence of Fe^{3+} and F^-

The results obtained through solution-based fluorescence measurements with the ligand **L_1** were interesting and highlight the potential of the ligand to selectively detect Fe^{3+} at low levels. Given the relevance of iron in cellular physiology and its biomedical implications, it was conceived that that compound **L_1** could perhaps be explored for fluorescence-based detection of intracellular Fe^{3+}. In this regard, determination of cytotoxic effect of compound **L_1** and **L_1-Fe** complex on model human cells was pertinent, prior to pursuing sensing applications in cells. To this end, HeLa cells were treated with varying concentrations of compound **L_1** and **L_1-Fe** complex for a period of 24 h and the cytotoxic effect of the test compounds were ascertained by MTT assay. As evident from Figure 8, the essential observation was that compound **L_1** as well as **L_1-Fe** complex did not induce any pronounced effect on the viability of HeLa cells. With increase in the concentration of the tested compound, a marginal reduction in cell viability was observed and even at the highest tested concentration of both the compounds (60 μM), the cell viability was nearly 80%. The viability of HeLa cells was not influenced by neither the solvent (DMSO) nor the iron salt, substantiating that the observed cytotoxic effect could be attributed to the ligand **L_1** and **L_1-Fe** complex.

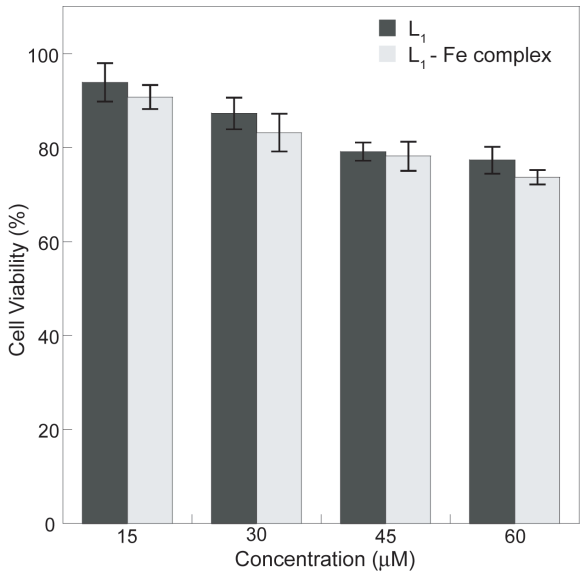

Fig. 8 MTT assay to determine the cytotoxic effect of compound **L_1** and **L_1-Fe** complex on HeLa cells.

Based on the results obtained in the cytotoxic assay, it was conceived that compound **L_1** at a concentration below 15 μM could be used for fluorescence-based imaging studies in order to detect **L_1-Fe** complex in live cells. To pursue this goal, HeLa cells were treated with 10 μM **L_1** solution for 1 h followed by incubation with 10 μM $Fe(NO_3)_3$ to allow the formation of **L_1-Fe** complex. From our previous optical as well as mass spectroscopic studies, the binding stoichiometry between **L_1** and Fe^{3+} was found to be 1:1, and hence it can be reasonably presumed that the concentration of **L_1-Fe** complex formed in HeLa cells would be much lower than the concentration (15

μM) at which a marginal cytotoxic effect of the complex was manifested (Figure 8).

Fluorescence microscope analysis revealed that HeLa cells treated with compound **L_1** alone failed to exhibit any fluorescence emission (Figure 9, Panel A). Interestingly, on incubation with $Fe(NO_3)_3$, a switch-ON fluorescence was conspicuous inside HeLa cells, which indicated the formation of **L_1-Fe** complex, as observed earlier in solution studies. It may also be mentioned here that the fluorescence was spread across the cell (Figure 9, Panel B).

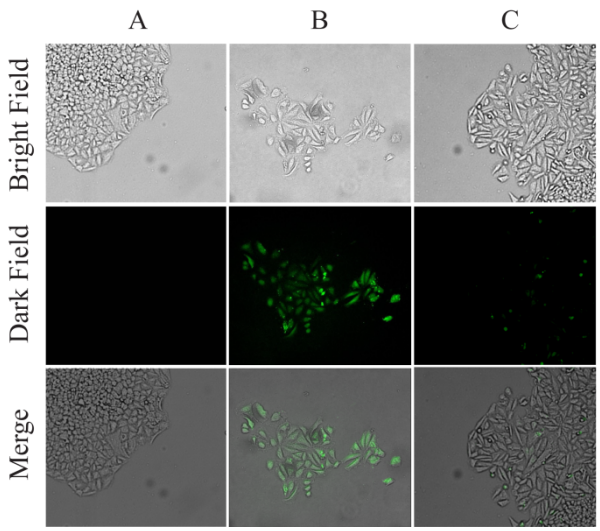

Fig. 8 Fluorescence microscopic images of HeLa cells (A) after treating with 10 μM **L_1**, (under blue light) (B) after adding 20 μM of Fe^{3+}, (under blue light) to the **L_1** treated cells (C) after adding 30 μM F^-, (under green light) to the (**L_1** + Fe^{3+}) treated cells. Scale bar for the images is 50 μm.

Fluoride sensing inside HeLa cells by **L_1-Fe** complex could also be pursued as evident from the notable switch-OFF of the green fluorescence emission inside cells following incubation with KF solution (Figure 9, Panel C). Collectively, the result obtained from fluorescence microscopic analysis indicated that compound **L_1** could cross the membrane barrier, infuse into HeLa cells and efficiently sense intracellular Fe^{3+} and F^- even in the complex cellular milieu. Bright field images of HeLa cells indicated that the treated cells exhibited the characteristic morphological traits, which also suggested that the cells were viable. Collectively the results reflect interesting prospect for future *in vivo* biomedical applications of the sensor.

Conclusion

In conclusion, we have developed a fluorophoric receptor **L_1** which selectively binds with Fe^{3+} ions and triggers a switch ON response in optical and fluorescence spectra in the visible region. The recognition behaviour of **L_1** is evaluated in presence of various competitive metal ions in mixed aqueous media. The detection limit for Fe^{3+} was found to be much lower than the permissible Fe^{3+} concentration in drinking water as per standard norms. Further, evaluation of the **L_1-Fe** complex prepared *in situ* demonstrated great promise for the detection of the Fe^{3+} ion in the presence of globular protein, serum and human serum albumin (HSA) solution. Anion dependent studies with **L_1-Fe** complex revealed that dissociation of the complex is possible selectively in presence of fluoride anion, which makes the **L_1-Fe** complex an efficient sensor for fluoride anions. The receptor **L_1** shows intense change in its fluorescence emission when bound to Fe^{3+} in physiological conditions. Hence, the effectiveness of compound **L_1** as a sensor for intracellular detection of Fe^{3+} by fluorescence microscopy was also studied. Moreover, the fluorescence microscopic analysis strongly suggested that compound **L_1** could readily permeate into HeLa cells and rapidly sense intracellular Fe^{3+} and F^-.

Acknowledgements

G.D. gratefully acknowledges Council of Scientific and Industrial Research (01/2727/13/EMR-II) and Science & Engineering Research Board (SR/S1/OC-62/2011), New Delhi, India, for financial support, CIF and IIT Guwahati for providing instrument facility. CK, SS, SM and BKD acknowledge IIT Guwahati for fellowship. We thank Department of Biotechnology, Government of India for a research grant (BT/01/NE/PS/08).

Notes and references

[a] Department of Chemistry, Indian Institute of Technology Guwahati, Assam, 781 039, India.
[b] Department of Biotechnology, Indian Institute of Technology Guwahati, Assam, 781 039, India.

Electronic Supplementary Information (ESI) available: 1H NMR, 13C NMR, and mass spectra as characterization data of L1 and L1-Fe complex. Benesi-Hildebrand plot, Job's plot, fluorescence intensity of the L1 solution in different protein solution and in presence and absence of Fe3+ ions. See DOI: 10.1039/b000000x/

1 A. P. de Silva, H. Q. N. Gunaratne, T. Gunnlaugsson , A. J. M. Huxley, C. P. McCoy, J. T. Rademacher and T. E. Rice, *Chem. Rev.,* 1997, **97**, 1515.
2 S. C. Burdette and S. J. Lippard, Coord. *Chem. Rev.,* 2001, **216**, 333.
3 D. T. McQuade, A. E. Pullen and T. M. Swager, *Chem. Rev.,* 2000, **100**, 2537.
4 B. Wang, J. Hai, Z. Liu, Q. Wang, Z. Yang and S. Sun, *Angew. Chem., Int. Ed.* 2010, **49**, 4576.
5 O. Oter, K. Ertekin, C. Kirilmis, M. Koca and M. Ahmedzade, *Sens. Actuators, B,* 2007, **122**, 450.
6 L. J. Fan and W. E. Jones, *J. Am. Chem. Soc.*, 2006, **128**, 6784.
7 J. Mao, L. N. Wang, W. Dou, X. L. Tang, Y. Yan and W. S. Liu, *Org. Lett.,* 2007, **9**, 4567.
8 C. R. Lohani and K. H. Lee, *Sens. Actuators, B*, 2010, **143**, 649.
9 R. S. Eisenstein, *Annu. Rev. Nutr.*, 2000, **20**, 627.
10 B. F. Matzanke, G. Muller-Matzanke and K. N. Raymond, Iron Carriers and Iron Proteins, VCH Publishers, New York, 1989, Vol. 5.
11 N. C. Andrews, *N. Engl. J. Med.*, 1999, **341**, 1986.
12 D. Touati, *Arch. Biochem. Biophys.*, 2000, **373**, 1.
13 E. Beutler, V. Felitti, T. Gelbart and N. Ho, *Drug Metab. Dispos.*, 2001, **29**, 495.
14 R. R. Crichton, Inorganic Biochemistry of Iron Metabolism: From Molecular Mechanisms to Clinical Consequences, 2nd ed., John Wiley & Sons, Chichester, 2001.
15 L. Ma, W. Luo, P. J. Quinn, Z. Liu and R. C. Hider, *J. Med. Chem.*, 2004, **47**, 6349.
16 R. Nudelman, O. Ardon, Y. Hadar, Y. Chen, J. Libman and A. Shanzer, *J. Med. Chem*., 1998, **41**, 1671.

17 H. Weizman, O. Ardon, B. Mester, J. Libman, O. Dwir, Y. Hadar, Y. Chen and A. Shanzer, *J. Am. Chem. Soc*., 1996, **118**, 12368.
18 D. P. Murale, S. T. Manjare, Y. S. Lee and D. G. Churchill, *Chem. Commun.*, 2014, **50**, 359.
19 D. P. Murale, A. P. Singh, J. Lavoie, H. Liew, J. Cho, H. I. Lee, Y. H. Suh, D. G. Churchill, *Sensors and Actuators B*, 2013, **185**, 755.
20 P. D. Beer and P. A. Gale, *Angew. Chem., Int. Ed.*, 2001, **40**, 486.
21 R. Martinez-Manez and F. Sancenon, *Chem. Rev.*, 2003, **103**, 4419.
22 E. Gazzano, L. Bergandi, C. Riganti, E. Aldieri, S. Doublier, C. Costamagna, A. Bosia and D. Ghigo, *Curr. Med. Chem*., 2010, **17**, 2431.
23 B. Spittle, Neurotoxic effects of fluoride, *Fluoride*, 2011, **44**, 117.
24 P. Grandjean and P. J. Landrigan, *Lancet*, 2006, **368**, 2167.
25 M. Cametti and K. Rissanen, *Chem. Commun.*, 2009, 2809.
26 S.-D. Jeong, A. Nowak-Krol, Y. Kim, S.-J. Kim, D. T. Gryko and C.-H. Lee, *Chem. Commun.*, 2010, **46**, 8737.
27 T. Mizuno, W.-H. Wei, L. R. Eller and J. L. Sessler, J. Am. Chem. Soc., 2002, **124**, 1134.
28 J. Ren, Z. Wu, Y. Zhou, Y. Li and Z. Xu, *Dyes Pigm*., 2011, **91**, 442.
29 P. Sokkalingam and C.-H. Lee, *J. Org. Chem.*, 2011, **76**, 3820.
30 Y. Qu, J. Hua and H. Tian, *Org. Lett*., 2010, **12**, 3320.
31 J. Wang, L. Yang, C. Hou and H. Cao, *Org. Biomol. Chem*., 2012, **10**, 6271.
32 I.-S. Ke, M. Myahkostupov, F. N. Castellano and F. P. Gabbai, *J. Am. Chem. Soc.*, 2012, **134**, 15309.
33 C. R. Cooper, N. Spencer and T. D. *Chem. Commun*., 1998, 1365.
34 T. W. Hudnall and F. P. Gabbai, *J. Am. Chem. Soc*., 2007, **129**, 11978.
35 H. N. Kim, M. H. Lee, H. J. Kim, J. S. Kim and J. Yoon, *Chem. Soc. Rev.*, 2008, **37**, 1465.
36 R. McRae, P. Bagchi, S. Sumalekshmy and C. J. Fahrni, *Chem. Rev*. 2009, **109**, 4780.
37 Z. Xu, J. Yoon and D. R. Spring, Fluorescent chemosensors for Zn2+, *Chem. Soc. Rev*., 2010, **39**, 1996.
38 R. P. Haugland, Handbook of Fluorescent Probes and Research Chemicals, 9th ed., Molecular Probes, Eugene, OR, 2002.
39 E. L. Que, D. W. Domaille and C. J. Chang, *Chem. Rev.*, 2008, **108**, 4328.
40 B. Valeur and I. Leray, *Chem. Rev.,* 2000, **205**, 3.
41 X. Peng, J. Du, J. Fan, J. Wang, Y. Wu, J. Zhao, S. Sun and T. Xu, *J. Am. Chem. Soc.,* 2007, **129**, 1500.
42 S. Adsule, V. Barve, D. Chen, F. Ahmed, Q. P. Dou, S. Padhye and F. H. Sarkar, *J. Med. Chem.,* 2006, **49**, 7242.
43 N. Aksuner, E. Henden, I. Yilmaz and A. Cukurovali, *Sensors and Actuators B,* 2008, **134**, 510.
44 N. Aksuner, E. Henden, I. Yilmaz and A. Cukurovali, *Dyes and Pigments,* 2009, **83**, 211.
45 Z. Yang, M. She, J. Zhang, X. Chen, Y. Huang, H. Zhu, P. Liu, J. Li and Z. Shi, *Sensors and Actuators B*, 2013, **176**, 482.
46 L. Yang, W. Zhu, M. Fang, Q. Zhang and C. Li, *Spectrochimica Acta Part A: Molecular and Biomolecular Spectroscopy*, 2013, **109**, 186.
47 M. Kumar, J. N. Babu and V. Bhalla, *J Incl Phenom Macrocycl Chem*., 2010, **66**, 139.
48 L. Tang, F. Li, M. Liu and R. Nandhakumar, *Spectrochimica Acta Part A*, 2011, **78**, 1168.
49 C. Kar, M. D. Adhikari, A. Ramesh and G. Das, *Inorg. Chem*., 2013, **52**, 743.
50 C. Kar, A. Basu and G. Das, *Tetrahedron Lett*., 2012, **53**, 4754.
51 C. Kar, M. D. Adhikari, A. Ramesh and G. Das, *RSC Adv*., 2012, **2**, 9201.
52 C. Kar and G. Das, *J. Photochem. Photobiol. A–Chem*., 2013, **251**, 128.
53 B. K. Datta, C. Kar, A. Basu and G. Das, *Tetrahedron Lett*., 2013, **54**, 771.
54 B. K. Datta, S. Mukherjee, C. Kar, A. Ramesh and G. Das, *Anal. Chem*., 2013, **85**, 8369.
55 C. Kar, M. D. Adhikari, B. K. Datta, A. Ramesh and G. Das, *Sensors and Actuators B*, 2013, **188**, 1132.
56 S. Samanta, S. Goswami, A. Ramesh and G.Das, *Sensors and Actuators B*, 2014, **194**, 120.
57 D. Olson and W.B. Hamlin, *Clin. Chem*. 1969, **15**, 438.
58 C. G. Neochoritis, T. Zarganes-Tzitzikas, C. A. Tsoleridis, J. Stephanidou-Stephanatou, C. A. Kontogiorgis, D. J. Hadjipavlou-Litina and T. Choli-Papadopoulou, *Eur. J. Med. Chem.*, 2011, **46**, 297.
59 H. A. Benesi and J. H. Hildebrand, *J. Am. Chem. Soc.,* 1949**, 71**, 2703.
60 M. Kumar and A. Puri, *Indian J Occup Environ Med.,* 2012**, 16**, 40.
61 J. Kanner, J. B. German and J. E. Kinsella, *CRC Crit. Rev. Food Nutr.,* 1987, **25**, 317.
62 R. E. Brantley, S. J. Smerdson, A. J. Wilkinson, E. W. Singleton and S. O. Otson, *J. Biol. Chem.,* 1993, **268**, 6995.
63 P. Brown, O. Shalev and R. P. Hebbel, *Free Radical Biol. Med.,* 1998, **24**, 1040.
64 S. R. Riberov and P. G. Bochev, Biochemistry and Biophysics, 1982, **213**, 288.
65 H. Nick, *Curr. Opin. Chem. Biol.,* 2007**, 11**, 419.
66 C. Hershko, G. Link and A. M. Konijn, Iron Chelation. In Molecular and Cellular Iron Transport; Templeton, D. M., Ed.; Marcel Dekker, Inc.: New York, 2002; 787.
67 M. Kumar, R. Kumar, V. Bhalla, P. R. Sharma, T. Kaur and Y. Qurishi, *Dalton Trans*., 2012**, 41**, 408.